Linear stability and receptivity analyses of the Stokes layer produced by an impulsively started plate

Paolo Luchini[a)]
Dipartimento di Ingegneria Aerospaziale, Politecnico di Milano, Via La Masa 34, 20158 Milano, Italy

Alessandro Bottaro
Institut de Mécanique des Fluides de Toulouse, Allée du Professeur Camille Soula, 31400 Toulouse, France

(Received 23 August 2000; accepted 2 March 2001)

The stability and the receptivity of the boundary layer produced by the impulsive motion of a flat plate in its plane is studied. The evolution of two-dimensional traveling disturbance waves for this physical situation, known as Stokes' first problem, is treated by integrating directly the (parabolic in time) linearized Navier–Stokes equation and by a multiple-scale approach. In the asymptotic analysis, the Orr–Sommerfeld equation is found at leading order. Through the compatibility condition for the equation at next order, an $O(1)$ correction to growth rates and frequencies is achieved. Such corrections are found to be very mild. After having established that the leading-order results are adequate when looking at the stability characteristics of the flow for a given (large) time, a receptivity analysis is performed. The adjoint of the parabolic system is obtained, and through its backward-in-time integration, the initial and wall Green's functions are obtained. These are then compared to the results of the multiple-scale receptivity analysis. © *2001 American Institute of Physics.* [DOI: 10.1063/1.1369605]

I. INTRODUCTION

We consider the flow induced by a flat plate initially at rest in a quiet medium and impulsively set in a motion parallel to itself at a constant speed U_∞, a situation commonly known as ''Stokes' first problem'' (e.g., Schlichting[1]) or ''Rayleigh problem'' (e.g., Panton[2]). This flow can be seen as analogous to the Blasius flow, with time being here the ''streamwise'' direction of evolution; it becomes linearly unstable after a *critical time* when two-dimensional Tollmien–Schlichting-like waves appear and occupy the whole horizontal (x) space. However, in contrast to the Blasius flow, the evolution of instabilities in Stokes' first problem is exactly described by a parabolic equation, whose numerical solution can be obtained relatively quickly and with no uncertainty as to the appropriate initial and boundary conditions. It is therefore an ideal test bed for asymptotic techniques of stability analysis.

The Stokes layer generated by a moving plate is also the flow produced behind a weak shock wave that propagates in a shock tube, when viewed in wall-fixed coordinates. Shock tubes are interesting in that they allow extreme operating conditions—high stagnation enthalpies—and are often used for studying transient aerodynamic effects. The assessment of shock tubes, and in particular the estimate of the transition time before turbulent flow sets in, has been the subject of several investigations (see e.g., Hartunian *et al.*[3] and Dillon and Nagamatsu[4]). However, this is not an easy task and, for example, the surface finish of the shock tube walls—an issue related to the flow receptivity—has a strong influence on the onset of transition. Myerson[5] reported that ''the same experiments performed in a honed (very smooth) shock tube of seamless stainless steel showed considerably longer times before reaching the transition from laminar to turbulent boundary layer, than did the previous tube in which the inner surface was left with the rough surface from the fabrication (extrusion) process.'' This seems at odds with what was reported by Aoki *et al.*[6] for which, apparently, ''transition propagates from the edge of the boundary layer to the wall.'' The matter clearly deserves further work; although the analogy with Stokes' first problem is strictly valid for weak shocks only, an understanding of the stability and receptivity properties of Stokes' problem may be useful. On the other hand, weak shocks are indeed encountered in railway tunnels.[7] When a high speed train enters a tunnel it gives rise to a pressure disturbance that precedes the train in the form of a weak shock and abruptly sets still air into motion. The boundary layer behind such a shock is described by Stokes' first problem. Since the walls of typical railway tunnels are not smooth, disturbance waves are expected to be triggered by the surface inhomogeneities (this is the receptivity step) and to be exponentially amplified (linear stability step).

The work on the stability of Stokes' first problem appears to have been initiated by Otto[8] who found good agreement between local (in time) Orr–Sommerfeld results and triple-deck solutions in regimes of common validity. The results were further extended by Webb *et al.*[9] who conducted linear and nonlinear marching (in time) calculations. Closely related studies include plane Couette flow during its startup phase from rest, and the decaying stages of the plane Couette flow, when the moving wall is suddenly stopped. In both situations, strictly local viscous analyses were carried

[a)]Present address: Dipartimento di Ingegneria Meccanica, Università di Salerno, 84084 Fisciano (SA), Italy.

out,[10,11] i.e., the mean flow at each instant was regarded as stationary. Despite this approximation, excellent agreement between the measured and the predicted most amplified wavelengths was reported by Tillmark and Alfredsson.[11] This is due to the fact that the base boundary layer flow, about which small disturbances are imposed, depends *slowly* on time, since there is a slow diffusion of vorticity from the plate outward to the medium. The disturbances evolve on a fast time scale so that the problem appears to be naturally amenable to an asymptotic approach based on separation of scales, which yields, at leading order, the strictly local (''frozen flow'') stability equations.

A multiple-scale technique is customarily applied to the study of the stability of spatially evolving boundary layers (see, e.g., Bouthier,[12,13] Gaster,[14] Saric and Nayfeh,[15] and Itoh[16]). The main difference with the problem studied here is that Stokes' problem remains parabolic in its exact formulation (no approximation of the PSE type[17] is needed for the study of this temporally developing boundary layer) and hence exempt from the uncertainties due to the ellipticity of the corresponding spatial problem. This bears more particularly on the receptivity aspects of the problem. While the exact parabolic nature of the temporal model allows treatment of the solution at and around $t=0$, the PSE often adopted for the analysis of the spatial problem cannot be used in proximity of the leading edge. It is hoped that an understanding of the initial receptivity of Stokes' first problem—besides its intrinsic interest—could also shed some light onto its spatial counterpart. In closing this section we note that Hill[18] used a local adjoint technique to establish the influence of inhomogeneous wall conditions and source terms in the equations in exciting two-dimensional Tollmien–Schlichting waves in the Blasius flow. A similar—nonlocal—technique has been adopted by Luchini and Bottaro[19] for the case of Görtler vortices developing over a concave wall boundary layer.

II. THE STABILITY PROBLEM

If an infinitely long flat plate is suddenly set into motion in its plane at a constant velocity the ensuing boundary layer flow satisfies the equations

$$U_x=0, \tag{1a}$$

$$U_t=\nu U_{yy}, \tag{1b}$$

$$V=0, \tag{1c}$$

with $U=U_0$ at $y=0$ and $U=0$ for $y\to\infty$. In the more general case, the outer velocity need not vanish, such as in the inviscid region behind a moving shock. For the sake of definiteness, however, we limit ourselves to the case of the undisturbed outer flow, bearing in mind that the more general situation of a constant $U\neq 0$ for $y\to\infty$ can always be reduced to the present one by a change of reference frame. A well known similarity solution of Eq. (1) was given by Stokes and takes the form

$$\frac{U}{U_0}=1-\mathrm{erf}(\eta), \tag{1d}$$

where the similarity variable η is taken to be $\eta=y/2\delta(t)$, with $\delta(t)=(\nu t)^{1/2}$ characteristic length.

The nondimensional linearized perturbation equations are

$$u_x+v_y=0, \tag{2a}$$

$$\frac{1}{\mathrm{Re}_0}u_t+Uu_x+vU_y+p_x-\frac{1}{\mathrm{Re}_0}(u_{xx}+u_{yy})=0, \tag{2b}$$

$$\frac{1}{\mathrm{Re}_0}v_t+Uv_x+p_y-\frac{1}{\mathrm{Re}_0}(v_{xx}+v_{yy})=0, \tag{2c}$$

with (u,v) disturbance velocity vector, with components along the streamwise x and the vertical y axis, and p disturbance pressure. In this work, to limit the number of parameters, we consider two-dimensional disturbances only. For the nondimensionalization, U_0 has been employed as velocity scale, t_0—a reference time—as time scale, $\delta_0=(\nu t_0)^{1/2}$ as length scale, and ρU_0^2 as pressure scale. Hence, a Reynolds number $\mathrm{Re}_0=U_0\delta_0/\nu=U_0(t_0/\nu)^{1/2}$ arises naturally. It is convenient to introduce a perturbation stream function ψ so that system (2) becomes

$$\frac{1}{\mathrm{Re}_0}\Delta\psi_t+U\Delta\psi_x-U_{yy}\psi_x-\frac{1}{\mathrm{Re}_0}\Delta^2\psi=0, \tag{3}$$

with $\psi=\psi_y=0$ for $y=0$, $y\to\infty$. Equation (3) is parabolic in time and can be solved subject to an initial condition at the initial time. Hence, the short-time behavior is a function of the initial state, but for sufficiently large times a common asymptotic limit is achieved.[9]

A. Marching and multiple-scale formulations

Equation (3) can be Fourier transformed in x by assuming that ψ varies like

$$\psi(t,x,y)=f(t,y)\exp[i\alpha_0 x], \tag{4}$$

and $\alpha_0=\alpha\,\delta_0$ denotes the dimensionless streamwise wave number. Equation (3) then becomes

$$\left[U-\frac{i}{\alpha_0\,\mathrm{Re}_0}\frac{\partial}{\partial t}\right](D^2-\alpha_0^2)f-U_{yy}f+\frac{i}{\alpha_0\,\mathrm{Re}_0}(D^2-\alpha_0^2)^2f=0, \tag{5a}$$

and it needs to be solved together with boundary conditions

$$f=f_y=0 \quad \text{for } y=0 \text{ and } y\to\infty. \tag{5b}$$

Equations (5) represent the marching formulation, which for this problem is an exact one.

Alternatively, a multiple-scale approximation can be set up when the disturbance behaves as a fast exponential $\exp[-i\alpha_0\varphi(t)/\epsilon]$. The scale factor ϵ can be determined by requiring that the dominant terms in Eq. (3) be of comparable magnitudes. Classically, by requiring that $(1/\mathrm{Re}_0)\Delta\psi_t=O(U\Delta\psi_x-U_{yy}\psi_x)$, and introducing the fast time scale $\tau=t/\epsilon$, the scaling parameter $\epsilon=\mathrm{Re}_0^{-1}$ emerges. However, since a straightforward expansion in powers of Re_0^{-1} would lead to a differential equation of reduced order (the Rayleigh equation) which is not uniformly valid across the boundary layer, we include some terms formally of order ϵ but locally

larger in the leading-order equation. This procedure, discussed among others by Gaster,[14] is legitimate with the understanding that the asymptotic series (6) in powers of ϵ, now becomes an *asymptotic sequence* of unknown—and decreasing—functions of ϵ.[20] The alternative to this approach—the solution of the Rayleigh equation together with a treatment of the inner and outer viscous layers[21]—would have considerably delayed the convergence of the approximation with increasing Reynolds number. On the other hand, the recent analysis by Govindarajan and Narasimha[22] of the spatial problem shows that the scaling indicated by the multiple-deck approach can indeed be incorporated into a multiple-scale approximation where ϵ is a combination of nonintegral powers of Re_0 and α_0.

When $\epsilon = 1/\mathrm{Re}_0$, a Wentzel–Kramers–Brillouin-type asymptotic expansion can be set up in the form

$$f(t,y) = \exp[-i\alpha_0 \varphi(t)/\epsilon][f_0(t,y) + \epsilon f_1(t,y) + \ldots], \tag{6}$$

where the first factor on the right-hand side accounts for the rapid growth and oscillation of f in time, whereas the second term accounts for the slow temporal evolution. Inserting (6) into (5a) and collecting like powers of ϵ we obtain

$$O(\epsilon^0): \quad [U-c(t)](D^2-\alpha_0^2)f_0 - U_{yy}f_0 + \frac{i}{\alpha_0 \mathrm{Re}_0}(D^2-\alpha_0^2)^2 f_0 = 0, \tag{7a}$$

$$O(\epsilon): \quad [U-c(t)](D^2-\alpha_0^2)f_1 - U_{yy}f_1 + \frac{i}{\alpha_0 \mathrm{Re}_0}(D^2-\alpha_0^2)^2 f_1 = \frac{i}{\alpha_0}(D^2-\alpha_0^2)f_{0,t}, \tag{7b}$$

with the phase velocity $c(t)$ defined by $c(t) = d\varphi(t)/dt = c_r(t) + ic_i(t)$. At leading order (the ''geometrical optics'' approximation of wave theory) we have the Orr–Sommerfeld equation, while at first order (the ''physical optics'' approximation) we have a forced Orr–Sommerfeld equation that can be solved under the condition

$$f_0^+ \cdot (D^2-\alpha_0^2)f_{0t} = 0, \tag{8}$$

with $\cdot$ denoting inner product, and f_0^+ being the eigenfunctions of the adjoint homogeneous problem. The Stokes' flow is parallel for all times, but unsteady, with the unsteadiness playing the role of the nonparallelism of the corresponding spatial problem. Incidentally, in this paper the term ''nonparallelism'' is often used in place of ''unsteadiness'' to indicate that the base flow evolves and is not frozen.

The solutions f_0 of Eq. (7a) are given by the product of an amplitude function $A(t)$ times the appropriately normalized direct eigenfunctions $f_d(t,y)$. Hence, by adopting the conventional definition of inner product over the space of complex-valued differentiable functions in $y \in [0,\infty)$, i.e.,

$$a \cdot b = \int_0^\infty \overline{a} b \, dy, \tag{9}$$

with the overbar meaning complex conjugate, the solvability condition (8) leads to

$$A(t) = A_0 \exp\left(-\int_{t_0}^{t} \frac{q_2(\tau)}{q_1(\tau)} d\tau \right),$$

with

$$q_1(t) = \int_0^\infty \overline{f_0^+}(D^2-\alpha_0^2) f_d \, dy$$

and

$$q_2(t) = \int_0^\infty \overline{f_0^+}(D^2-\alpha_0^2) f_{d,t} \, dy.$$

The (arbitrary but uninfluential) normalization chosen for the eigenfunctions of (7a) in $y \in [0,\infty)$ and $\forall t$ is

$$\int_0^\infty (|f_{d,y}|^2 + \alpha_0^2 |f_d|^2) dy = 1. \tag{10}$$

In addition, a phase for each eigenfunction has been fixed by imposing that $f_{d,yy}(0)$ be a positive real number. It should be noted that the solution f_0 becomes unique and independent of the normalization of f_d once the first-order compatibility condition is imposed.

A local complex phase velocity of the exact solution c^{ex}, to be used for comparison with the asymptotic results, can be defined as

$$c^{\mathrm{ex}}(t) = c_r^{\mathrm{ex}}(t) + ic_i^{\mathrm{ex}}(t) = \frac{i\epsilon}{2E\alpha_0} \int_0^\infty \overline{u}\frac{\partial u}{\partial t} + \overline{v}\frac{\partial v}{\partial t} dy,$$

with E disturbance kinetic energy given by

$$E = \frac{1}{2}\int_0^\infty (|u|^2 + |v|^2) dy. \tag{11}$$

The imaginary part c_i^{ex} of c^{ex} is related to the growth rate of the instability

$$c_i^{\mathrm{ex}}(t) = \frac{\epsilon}{2E\alpha_0}\frac{\partial E}{\partial t}.$$

Both the real and imaginary parts of c^{ex} can be compared with the corresponding quantities from the multiple-scale analysis, which at the geometrical optics level are just the real and imaginary parts of c, and at the physical optics approximation are

$$c_i^{\mathrm{po}} = c_i - \epsilon \,\mathrm{Real}\left[\frac{q_2(t)}{\alpha_0 q_1(t)}\right] + O(\epsilon^2), \tag{12a}$$

$$c_r^{\mathrm{po}} = c_r + \epsilon \,\mathrm{Imag}\left[\frac{q_2(t)}{\alpha_0 q_1(t)}\right] + O(\epsilon^2), \tag{12b}$$

because in the latter approximation the energy has become

$$E = |A \exp[i\alpha_0(x - \varphi(t)/\epsilon)]|^2$$

with the normalization (10) understood. Clearly, a different normalization would introduce an additional, small $O(\epsilon)$ correction to (12) without changing the physical result.

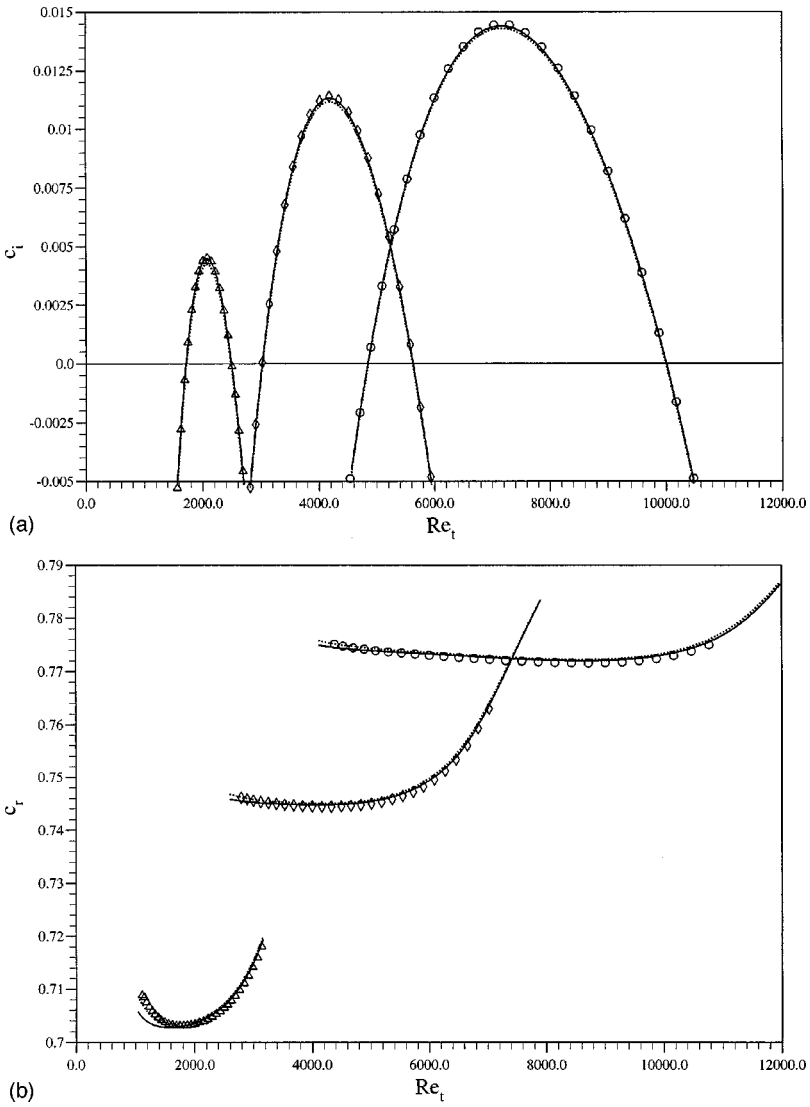

FIG. 1. (a) Amplification factor as a function of Re_t for, from left to right, $P=10^{-4}$, 4×10^{-5}, and 2×10^{-5}. (b) Phase speed.

B. Numerical solution technique and stability results

Both Eqs. (5a) and (7a) with their boundary conditions are discretized by fourth-order compact finite differences in y. The outer boundary is set at $y_\infty=20$, where the standard asymptotic condition of inviscid outer behavior is enforced. The marching equation is solved by a fully implicit method using second-order backward differences in t; the eigenvalue problem by inverse iteration. Problem (7a) is also solved by a spectral collocation procedure and the eigenvalue c of largest imaginary part is found in agreement with any desirable precision between the two approaches, when a sufficient number of finite difference nodes and Chebyshev collocation points are used. To solve the equation adjoint to (7a) we simply determine, using the same inverse-iteration process, the left eigenvector corresponding to the same eigenvalue of the generalized eigenvalue problem $Af_0=cBf_0$ [a symbolic form of (7a)]. The numerical integration starts from a small value of t (often $t=0.1$) and marches in time in (typically) 100 nonuniform steps up to $t=1$. Thus, the reference time used to define Re_0 and α_0 is the final time, and the local Reynolds number and wave number for smaller times vary as $\mathrm{Re}_t=\mathrm{Re}_0\,t^{1/2}$ and $\alpha_t=\alpha_0 t^{1/2}$. Both the ''parallel'' $(O(\epsilon^0))$ and the ''nonparallel'' $(O(\epsilon^1))$ terms in (12) are computed at all times.

A dimensionless wave number which does not contain the arbitrary reference time t_0 can be defined as

$$P=\alpha_t/\mathrm{Re}_t=\alpha_0/\mathrm{Re}_0=\alpha\nu/U_0,$$

with α the dimensional wave number. Similarly to the frequency parameter $F=\omega\nu/U_0^2$ normally used in presenting spatial stability results, P is a constant during the evolution of any one instability mode and is a small number of the order of 10^{-5} in the interesting range where disturbances are amplified.

In Fig. 1 we show the time evolution of c_i and c_r for three values of P. Dotted lines represent the strictly local results, continuous lines are the first order (physical optics) solutions, while the symbols pertain to simulations of the marching equation (5) started at $t=0$ with an impulse disturbance at the wall. The agreement in c_i and c_r between the exact solution and the nonparallel values provided by the multiple-scale analysis is excellent for t large enough for the

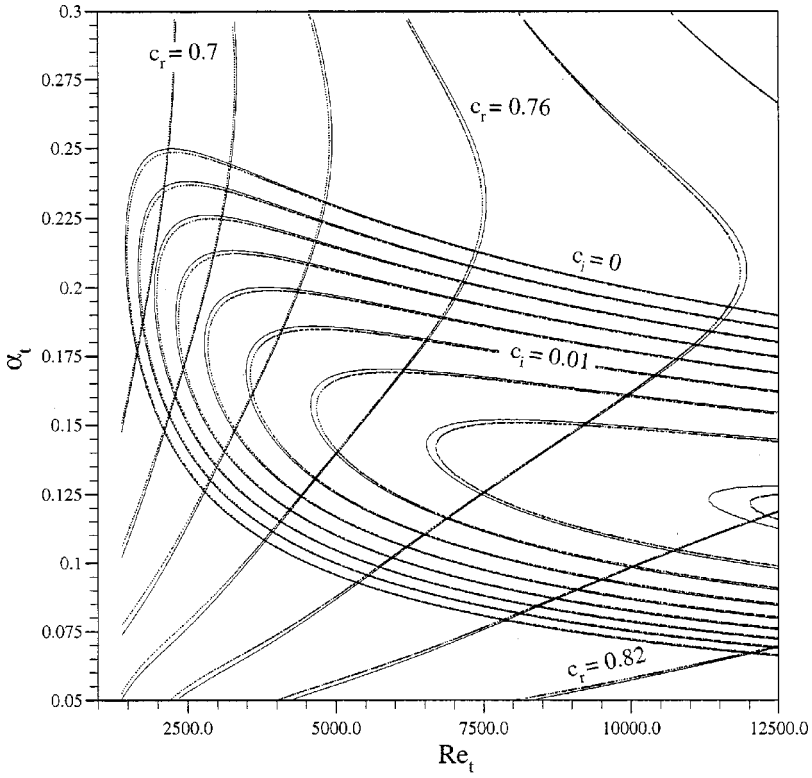

FIG. 2. Curves of constant phase speed and growth rate. Dotted lines correspond to local solutions (c_r, c_i), while solid lines indicate non-parallel results $(c_r^{\mathrm{po}}, c_i^{\mathrm{po}})$.

initial transient in the marching solutions to have died out. The growth rate is seen at first to increase, to peak, and then to decrease, just like in the case of the Blasius boundary layer.

Curves of constant amplification factor c_i and phase speed c_r in the $(\mathrm{Re}_t, \alpha_t)$ plane are given in Fig. 2. Also these curves resemble the corresponding ones for the Blasius flow and the nonparallel correction to the strictly local results is very small. The critical conditions from the local solutions are found to be

$$\mathrm{Re}_{\mathrm{crit}} = 1485.68, \quad \alpha_{\mathrm{crit}} = 0.2128, \quad c_{r\,\mathrm{crit}} = 0.686\,45,$$

in excellent agreement with those reported by Otto[13] which were, respectively, 1484.2, 0.2128, and 0.6865. Like in the case of the Blasius boundary layer, nonparallel estimates of the critical Reynolds number produce slightly lower values, and in the present case physical optics results are

$$\mathrm{Re}_{\mathrm{crit}} = 1456.72, \quad \alpha_{\mathrm{crit}} = 0.2139, \quad c_{r\,\mathrm{crit}} = 0.684\,74.$$

The phase speed is also reasonably close to the critical phase speed for the Blasius boundary layer, which in the reference frame of the outer stream is $1-0.39=0.61$. To set ideas, if the medium in which the plate moves is, say, air, and $U_0 = 10\,(\mathrm{m/s})$, after a time $t_c = \mathrm{Re}_{\mathrm{crit}}^2 \nu / U_0^2 \approx 0.33\,(\mathrm{s})$, Tollmien–Schlichting waves of streamwise wavelength $\lambda_c = 2\pi(\nu t_c)^{1/2}/\alpha_{\mathrm{crit}} \approx 0.067\,(\mathrm{m})$ and frequency $f_c = (1/2\pi)\omega_{\mathrm{crit}} U_0 (\nu t_{\mathrm{crit}})^{-1/2} \approx 590\,(\mathrm{Hz})$ become amplified. The stream function shape f_d of the mode corresponding to the local critical conditions is represented in Fig. 3, together with the corresponding solution from the marching equations. As expected, the peak in f_d is shifted towards the edge of the Stokes layer ($\delta_{99} \approx 4$), and so is the critical layer. At each value of the Reynolds number there are only a few discrete eigenmodes, together with a continuous spectrum of damped modes with $c_r = 0$.

III. RECEPTIVITY IN THE MULTIPLE-SCALE FORMULATION

Receptivity of amplified modes to external disturbances is generally calculated, in a parallel setting, by Laplace transform techniques (e.g., Crouch,[23] Hill,[18] Tumin,[24] Ashpin and Reshotko[25]). In the present problem this would mean endowing Eq. (5) with a nonzero forcing term, Laplace transforming both sides with respect to time, solving the resulting one-dimensional problem in the transformed domain, and then reducing the inverse-transform complex integral to a sum of residues over the dominant poles. The poles of the solving kernel correspond to the eigenvalues of the associated homogeneous problem, and the residues of simple poles split into the product of direct and adjoint eigenfunctions (i.e., eigenfunctions of the adjoint differential problem). The adjoint eigenfunctions therefore become projectors of the external forcing onto the corresponding direct mode.

The above procedure, however, does not produce a one-dimensional eigenvalue problem if the underlying base flow is time dependent (nonparallel in a spatial setting). In fact, in this case the Laplace transform produces a two-dimensional integrodifferential equation, which is even more intractable than the original. This approach was nonetheless found to give useful results[26] if the base flow is linearized with respect to the longitudinal coordinate in a neighborhood of a roughness element and the Laplace-transformed equation is solved perturbatively. The resulting solution, however, is not uni-

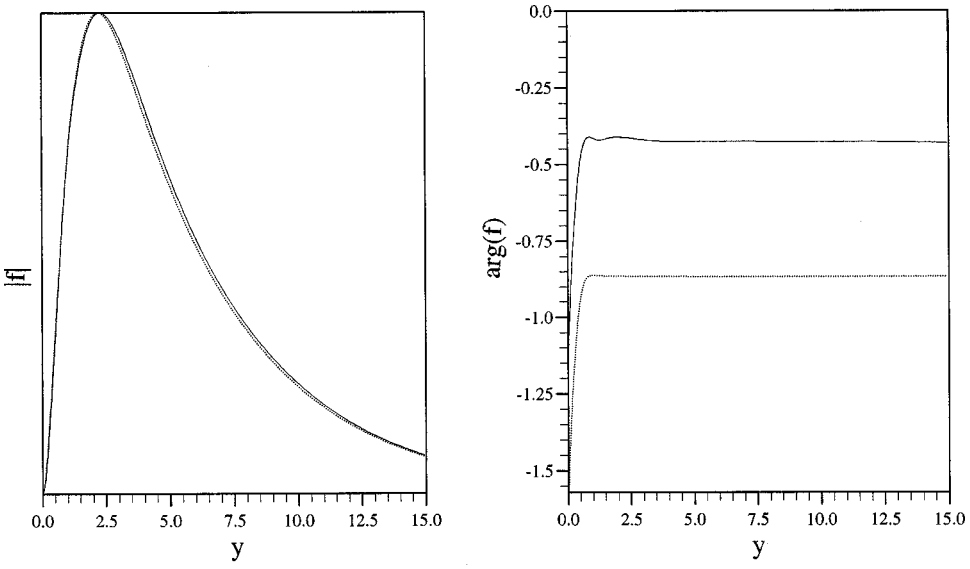

FIG. 3. Modulus (left) and phase of the disturbance stream function for $\alpha_0=0.2128$ and $\mathrm{Re}_0=1485.68$. Solid lines denote the marching solution, while the local eigensolution is plotted with dotted lines.

formly valid downstream of the roughness element, because of the secular behavior which typically affects perturbative solutions to oscillation problems. This situation is well known in wave-propagation theory (e.g., Whitham[27]), where evaluation of Laplace integrals provides small-wavelength asymptotics in homogeneous media, but direct multiple-scale expansions of the differential problem are used for weakly inhomogeneous media. Therefore, to generalize the results of previous authors (who replaced the boundary layer by a parallel flow with the same local profile in order to be able to apply a Laplace transform) and produce a uniformly valid asymptotic expansion capable of providing higher-order nonparallel corrections, we shall resort to a multiple-scale formulation of the receptivity problem. This will now be formulated for the time-growing Stokes layer, but with an eye to keeping it general enough that it can also be applied to space-evolving flows.

If problem (5) is modified by an inhomogeneous known term, either in the differential equation or in the boundary conditions, we may still assume that the solution behaves approximately as $\exp[-i\alpha_0\varphi(t)/\epsilon]$ provided the known term is $O(\epsilon)$, say $-(i/\alpha_0)\epsilon\, s(y,t)$. In fact in this case, under the same assumption of an expansion in the form of Eq. (6), Eq. (7a) is unchanged. Equation (7b) on the other hand acquires an additional source term and the compatibility condition (8) becomes

$$f_0^+ \cdot \{(D^2-\alpha_0^2) f_{0,t} - s(y,t)\exp[i\alpha_0\varphi(t)/\epsilon]\} = 0. \tag{13}$$

On assuming, as before, that f_0 is the product of an amplitude factor $A(t)$ times the appropriately normalized direct eigenfunction $f_d(t,y)$, Eq. (13) can be read as a first-order linear differential equation for $A(t)$, namely,

$$q_1 dA/dt + q_2 A = f_0^+ \cdot s(y,t)\exp[i\alpha_0\varphi(t)/\epsilon], \tag{14}$$

which has an elementary analytical solution. Thus the product of the adjoint eigenfunction and the source term emerges naturally. Equation (14) if applied to a time-independent problem with q_1 and f_0^+ independent of time, $\varphi(t)$ linear and q_2 equal to zero, gives the same result as the Laplace-transform approach. With respect to just replacing a nonparallel problem by a parallel one with the same local profile, however, Eq. (14) already contains first-order nonparallel corrections, in the form of the term $q_2 A$, which has no equivalent in the local approach, and can be continued to higher orders in ϵ with no conceptual nor practical difficulty. This is just as well, because replacing time by space and applying the same reasoning to a spatial stability problem poses no difficulty.

IV. EXACT ADJOINT FORMULATION OF THE RECEPTIVITY PROBLEM: MARCHING BACKWARD IN TIME

Having established that a unique functional form (a normal mode) is obtained for t sufficiently large, we now set to formulate the receptivity problem, i.e., to study the way in which disturbances at the wall ($y=0$) and at $t=0$ produce this functional form. An exact technique of receptivity analysis perfectly suited for this task is the backward-in-time approach described by Luchini and Bottaro.[19] It relies on the integration of the (backward parabolic) adjoint stability equation from the final time ($t=1$) down to the initial time ($t=0$) where the instability normally originates. With a single integration of the adjoint equation, the wall receptivity functions and the receptivity to production terms in the equations are also obtained, at no additional cost. All of this is easily established by application of the Green–Lagrange identity[28,29] to Eq. (5), equipped, for generality, of inhomogeneous wall conditions, i.e., $f(0,t)=f_w(t)$ and $f_y(0,t)=g_w(t)$. By using the inner product (9), the adjoint equation is easily found to be

$$\left[U - \frac{i}{\alpha_0\,\mathrm{Re}_0}\frac{\partial}{\partial t}\right](D^2-\alpha_0^2)f^+ + 2U_y Df^+ - \frac{i}{\alpha_0\,\mathrm{Re}_0}(D^2-\alpha_0^2)^2 f^+ = 0, \tag{15a}$$

together with the boundary conditions

$$f^+ = f_y^+ = 0 \quad \text{for } y=0 \text{ and } y\to\infty. \tag{15b}$$

Furthermore, the following relation, arising from the time derivative and the boundary terms, must be satisfied:

$$\frac{d}{dt}[f\cdot(D^2-\alpha_0^2)f^+]+D^2f^+(0,t)\overline{g_w}(t)-D^3f^+(0,t)\overline{f_w}(t)=0. \tag{16}$$

Equation (16) is key to defining receptivities. To see it, note that direct integration of (5) yields at $t=1$ a normal mode, i.e., $f(1,y)=f_0(1,y)=A(1)f_d(1,y)$, with the normalization of the direct eigenfunction given by Eq. (10). The initial condition for the adjoint calculation is taken to be the local adjoint eigenfunction $f_0^+(1,y)$, normalized by

$$(D^2-\alpha_0^2)f_0^+(1,y)\cdot f_d(1,y)=1.$$

Hence, by integrating Eq. (16) in time the final amplitude $A=A(1)$ of the direct mode is immediately available:

$$A=\int_0^\infty f(0,y)G^{t=0}(y)dy+\int_0^t u_w(t)G_w^u(t) + v_w(t)G_w^v(t)dt, \tag{17}$$

with $G^{t=0}(y)=(D^2-\alpha_0^2)\overline{f^+}(0,y)$ the initial Green's function, and the u and v wall Green's function given, respectively, by $G_w^u(t)=-\overline{f_{yy}^+}(0,t)$ and $G_w^v(t)=-(i/\alpha_0)\overline{f_{yyy}^+}(0,t)$.

The Green's functions defined above are obtained by a single integration of (15), starting from $t=1$ and proceeding backward to the nonmodal region of very small t; these functions are of immediate use. If, for example, the wall boundary conditions are homogeneous (i.e., the wall is smooth, and no blowing/suction is applied to it), and if the initial condition at $t=0$ is such that $f(0,y)=\delta(y-y_0)$, the final amplitude of the mode produced by this initial condition is simply $A=G^{t=0}(y_0)$. Suppose now that initially no disturbances are present in the flow, and that a pointwise (in t) disturbance is provided in the vertical wall velocity, i.e., $v(t,0)=v_w(t)=\delta(t-t_s)$. In this case the final amplitude of the mode is $A=G_w^v(t_s)$. Clearly, if the initial and/or boundary conditions are distributed over y and/or t (and not pointwise like in the above examples), the scalar product (17) immediately provides the final amplitude. In closing the section we note that the Green's functions obtained from *one* backward-in-time calculation could also have been obtained from a large number of forward numerical integrations of (5).

A. The numerical implementation of the adjoint equation

In a discrete setting, the solution of a parabolic differential equation such as (5a) is obtained through a chain of (generally implicit) algebraic problems of the form

$$\mathbf{A}_{n+1}\mathbf{f}_{n+1}=\mathbf{B}_n\mathbf{f}_n+\mathbf{b}_n, \tag{18}$$

where subscript n numbers consecutive discrete instants of time, $\mathbf{f}_n$ is the numerical vector containing the discretized stream function at time n, and matrices $\mathbf{A}_{n+1}$ and $\mathbf{B}_n$ contain a representation of the differential problem in whatever computational scheme is chosen (fourth-order compact differences in y and Crank–Nicolson in time for the present). Both matrices may generally depend on the time index n (because the base flow does). Vector $\mathbf{b}_n$ contains the inhomogeneous boundary conditions at discrete time n and $\mathbf{f}_0$ the initial data at time 0.

The solution of Eq. (18) can be formally written as

$$\mathbf{f}_N=\mathbf{A}_N^{-1}(\mathbf{b}_{N-1}+\mathbf{B}_{N-1}\mathbf{A}_{N-1}^{-1}(\mathbf{b}_{N-2}+\mathbf{B}_{N-2}\mathbf{A}_{N-2}^{-1}(\ldots(\mathbf{b}_1 + \mathbf{B}_1\mathbf{A}_1^{-1}(\mathbf{b}_0+\mathbf{B}_0\mathbf{f}_0))\ldots))).$$

Now assume the final result at time $n=N$ is to be projected onto a given arbitrary vector $\mathbf{f}_N^+$ through the scalar product $A=\overline{\mathbf{f}_N^+}\mathbf{f}_N$ [discrete representation of (9)]. Then this product, explicitly written as

$$A=\overline{\mathbf{f}_N^+}\mathbf{A}_N^{-1}(\mathbf{b}_{N-1}+\mathbf{B}_{N-1}\mathbf{A}_{N-1}^{-1}(\mathbf{b}_{N-2} + \mathbf{B}_{N-2}\mathbf{A}_{N-2}^{-1}(\ldots(\mathbf{b}_1+\mathbf{B}_1\mathbf{A}_1^{-1}(\mathbf{b}_0+\mathbf{B}_0\mathbf{f}_0))\ldots))), \tag{19}$$

can more easily be calculated for arbitrary data $\mathbf{b}_n$ and $\mathbf{f}_0$ by working it out from left to right. In fact, Eq. (19) can obviously be written as a linear superposition of the boundary and initial data with suitable coefficients $\overline{\mathbf{b}_n^+}$ and $\overline{\mathbf{f}_0^+}$, namely

$$A=\sum_{n=0}^{N-1}\overline{\mathbf{b}_n^+}\mathbf{b}_n+\overline{\mathbf{f}_0^+}\mathbf{f}_0. \tag{20}$$

A direct comparison of Eqs. (19) and (20) then shows that the coefficients obey the following recursion relations:

$$\overline{\mathbf{b}_{n-1}^+}=\overline{\mathbf{f}_n^+}\mathbf{A}_n^{-1}; \quad \overline{\mathbf{f}_{n-1}^+}=\overline{\mathbf{b}_{n-1}^+}\mathbf{B}_{n-1}. \tag{21}$$

Equations (21) are, in fact, the discrete adjoint equations, wherefrom $\overline{\mathbf{b}_n^+}$ and $\overline{\mathbf{f}_n^+}$ can be obtained by iterating backwards from $n=N$ down to $n=0$, at the same computational cost as a single numerical solution of the forward problem. One can notice that, as just a few components of the vector $\mathbf{b}_n$ are generally nonzero in order to represent the boundary conditions at the wall, only the corresponding components of $\overline{\mathbf{b}_n^+}$ need to be permanently stored for the subsequent calculation of the final amplitude A from the scalar product (20).

Just as the backward-parabolic differential adjoint equation (15a), the discrete adjoint equation (21) must be equipped with an initial condition at the final time $n=N$. As is clear from the above argument, the most appropriate initial condition $\overline{\mathbf{f}_N^+}$ for the backward iteration (21) is the projector of the final state onto the mode whose amplitude is to be calculated, that is, if the final time is large enough for local eigenfunctions to be well established, the left eigenfunction of the local problem. However, if a single mode is locally amplified at the final time, just any initial condition $\overline{\mathbf{f}_N^+}$ that is not orthogonal to this mode is acceptable (as already noticed by Luchini and Bottaro[19] for the spatially parabolic Görtler problem). In fact, provided only that $\overline{\mathbf{f}_N^+}$ is normalized so that its scalar product with this mode equals unity, Eq. (20) will yield the final amplitude of the most amplified forward mode. This also means that, to the same degree of approximation that the direct solution tends to one and the same final shape, apart from an amplitude factor, for almost any initial condition at time zero, the adjoint solution as well shall tend

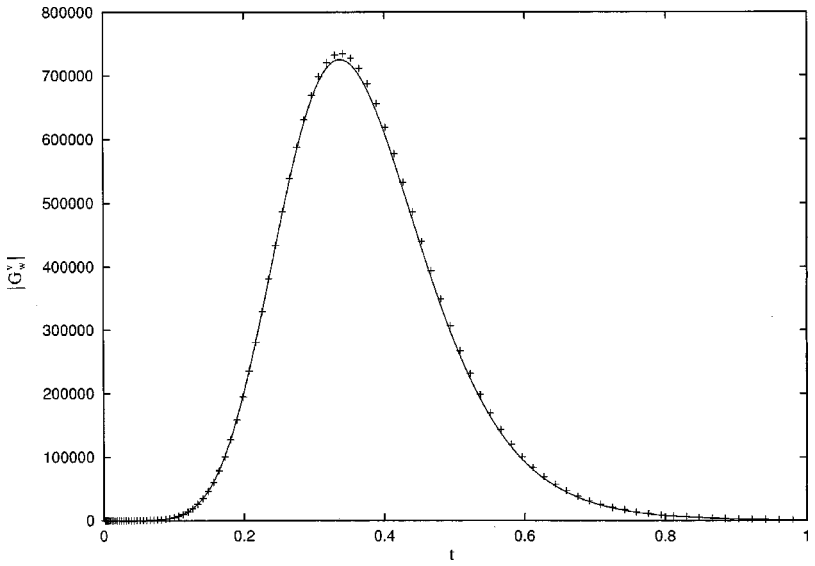

FIG. 4. Absolute value of the vertical-velocity receptivity G_w^v for $\alpha_0=0.2$ and $\mathrm{Re}_0=5000$. Symbols are used for the multiple-scale (order ϵ) results, the line corresponds to the exact (marching) solution.

to one and the same shape at time zero, apart from an amplitude factor which has to be fixed through normalization, for almost any initial condition at time N.

B. The wall Green's functions

By applying the backward-marching procedure detailed in the previous section and extracting from the vector $\overline{\mathbf{b}_n^+}$ the coefficients that multiply the values of $u=\psi_y$ and $v=-\psi_x$ at the wall, we can obtain a complete map of the receptivity to these two quantities. We can therefore quantify the effect of external disturbances that translate into nonzero values of velocity at the wall, either directly through active blowing and suction or wall vibration, or indirectly through imperfections of the wall geometry which can be represented in a perturbative setting by inhomogeneous velocity boundary conditions. The computation must be performed with a large number of time steps to allow for the oscillating character of the solution, but gives the exact wall receptivities of the most amplified instability, which can serve as a check on the much more quickly computed multiple-scale approximation of the same quantity presented in Sec. III.

For a wave number $\alpha_0=0.2$ and Reynolds number $\mathrm{Re}_0=5000$, corresponding to a time large enough that a sizeable amplification has taken place after the neutral point, Figs. 4 and 5 report the absolute values of the receptivities of the most amplified mode to normal and tangential velocity disturbances at the wall, calculated with both the multiple-scale formula (14) and the exact adjoint formulation. Both curves are normalized to a unit value of the final energy (11). In other words, they represent the amplification factor by which the wall velocity must be multiplied to produce the corresponding final amplitude (square root of the final energy). As may be seen, the agreement is very satisfactory, notwithstanding the fact that the multiple-scale result is 100 times faster to calculate.

To give a general picture of the time and wave number

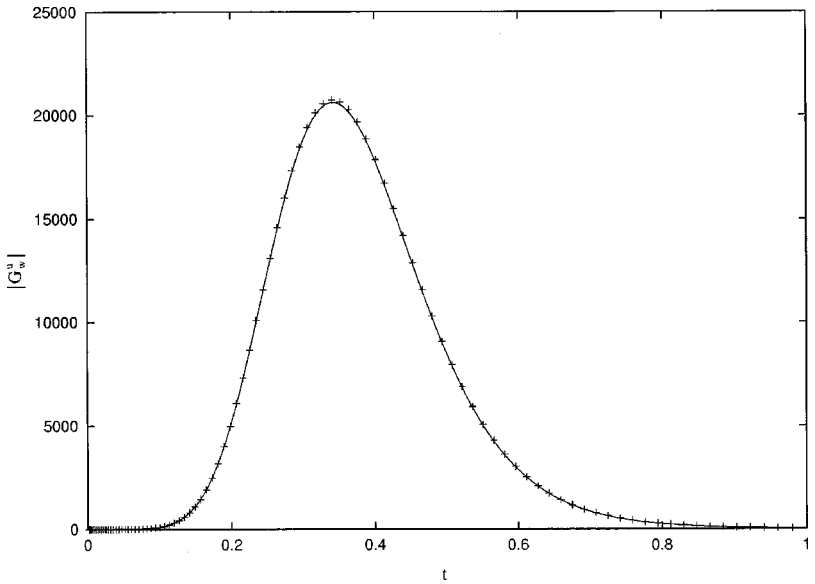

FIG. 5. Same as Fig. 4 for G_w^u.

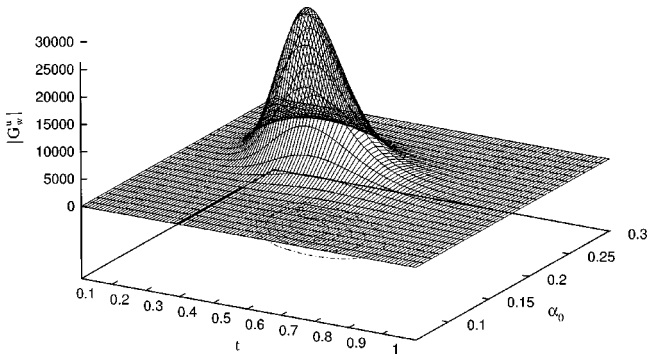

FIG. 6. Three-dimensional view of the absolute value of the receptivity to horizontal-velocity disturbances at the wall, $\mathrm{Re}_0=5000$.

distribution of wall receptivity, Fig. 6 shows a three-dimensional plot of the receptivity to tangential velocity disturbances. As may be expected, maximum receptivity occurs in a neighborhood of the neutral point, but in both the time and wavelength axes this neighborhood is broader than could be expected on the basis of the relatively large amplification involved. On the other hand, the receptivity, whose absolute value only has been plotted up to this moment, also involves a rapidly varying phase factor. This shows up in a plot of the Fourier transform of the previous result, that is the receptivity to disturbances of a given wave number and frequency rather than a given wave number and time of application. It turns out that the frequency response is very selective, and can only be poorly represented by a three-dimensional plot. A series of cross sections at discrete wave numbers are given instead in Fig. 7. As can be seen, the half-amplitude frequency band is about 3% of the center frequency.

C. The initial time Green's function

Just as inhomogeneous boundary conditions for Eq. (5) represent external disturbances appearing at the wall in the course of time, inhomogeneous initial conditions represent external disturbances already present in the whole flowfield at the time motion is started. A receptivity can be defined and calculated for these as well, which plays the same role as the leading-edge receptivity of a spatially evolving problem.

The initial time Green's function is much trickier to calculate than the wall Green's function, for these two reasons: (i) a multiple-scale approximation becomes invalid at small times and (ii) the result comes out of a balance between a large attenuation, taking place up to the neutral time, and a large amplification taking place afterward. Therefore, the total receptivity factor of the final mode to the initial disturbance is, like the difference of two large quantities, very sensitive to computation errors, and could only be reliably obtained with a very large number of time steps (of the order of 100 000 at $\mathrm{Re}=5000$). In addition, for any practically attainable Reynolds number the balance turns out to be in favor of damping, even if by analogy with the asymptotic estimates of Goldstein[30] for the spatially evolving boundary layer one could imagine that, with increasing and increasing Reynolds number, eventually amplification might win. This further complicates the matter, because it means that the mode that is eventually the fastest (and only) growing one receives but a small fraction of the initial disturbance.

A typical curve for the initial receptivity, at $\mathrm{Re}_0=5000$ and $\alpha_0=0.2$, is shown in Fig. 8. This is a stream function receptivity, that is the factor by which the initial stream function must be multiplied in order to give the final amplitude of the most amplified mode. The very fact that the numbers on this plot are on the order of 10^{-4} shows that the coupling of the eventually amplified mode with an initial disturbance is for all purposes negligible: the receptivity of this mode is even less than that of a disturbance traveling outside the boundary layer, which undergoes viscous dissipation without any interaction with the base flow.

Just as the leading-edge receptivity of a spatially evolving problem,[30] the initial receptivity of the Stokes layer can be split in an $O(1)$ nonmodal contribution, which can be calculated once and for all from a boundary-layer type equation, and a modal contribution, calculable within the

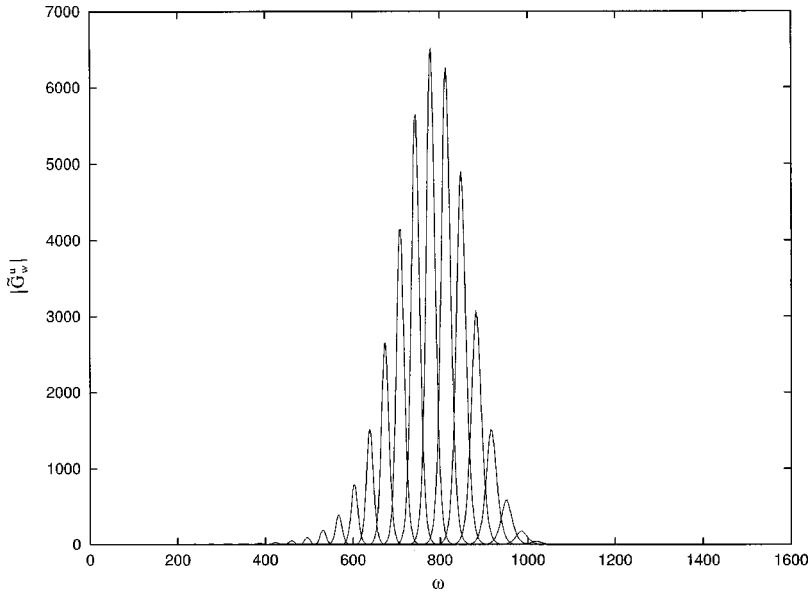

FIG. 7. Absolute value of the Fourier transform $\tilde{G}^u_w$ of G^u_w at different values of α_0.

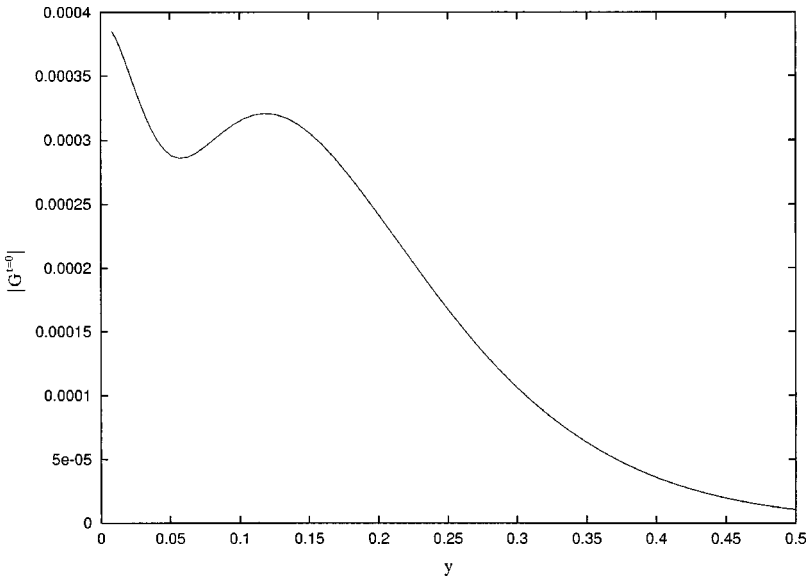

FIG. 8. Absolute value of the initial receptivity $G^{t=0}$ to stream function disturbances, $\alpha_0=0.2$, $\mathrm{Re}_0=5000$ ($P=4\times10^{-5}$).

multiple-scale approximation, which contains both the damping and the amplification stages. The nonmodal contribution to the receptivity can be formally obtained from Eq. (5) by letting the Reynolds number tend to infinity with $\alpha U_0 t_0$ and $y\sqrt{\alpha\nu/U_0}$ constant. In fact, for $t\gg(\alpha U_0)^{-1}$ the multiple-scale approximation of Sec. II applies, whereas for $t\ll(\alpha^2\nu)^{-1}$ terms containing α_0^2 are negligible in Eq. (5) and the solution becomes a function of the product $\alpha_0\,\mathrm{Re}_0$ only. The ratio of these two characteristic times, $U_0/(\alpha\nu)=P^{-1}$, is a large number in the region of parameter space where the instability is observed, and therefore the two limits overlap and a composite solution becomes possible. The composite solution is obtained by arbitrarily choosing a matching value t_M of $\alpha U_0 t$ and computing a multiple-scale amplification on one side from $t=t_M/(\alpha U_0)$ up to the actual final time t_0, and on the other the receptivity to initial disturbances of the amplitude at a time $T\gg t_M/(\alpha U_0)$ less its multiple-scale amplification for $t_M/(\alpha U_0)<t<T$. The result is of course independent of t_M and, if T were the final time t_0, it would give the exact receptivity. If, on the other hand, the second step is replaced by its limit for $P\to0$ with T such that simultaneously $\alpha U_0 T\to\infty$ and $\alpha^2\nu T\to0$, a universal receptivity curve is obtained. Such a curve, which applies for any sufficiently large Reynolds number and not just for $\mathrm{Re}_0=5000$, is shown in Fig. 9 for $t_M=\pi$.

V. SUMMARY AND CONCLUSIONS

A linear analysis of the stability and receptivity properties of the Stokes flow produced by a flat plate suddenly put in a motion parallel to itself in a previously quiescient medium has been conducted. The characteristic parameter of the analysis is a Reynolds number based on time and the instability sets in after a critical time, in close analogy to the case of the Blasius boundary layer for which Tollmien–Schlichting waves are amplified beyond some critical length. Just like in this latter flow situation, the amplification factor of the present instability first grows and then decreases at any

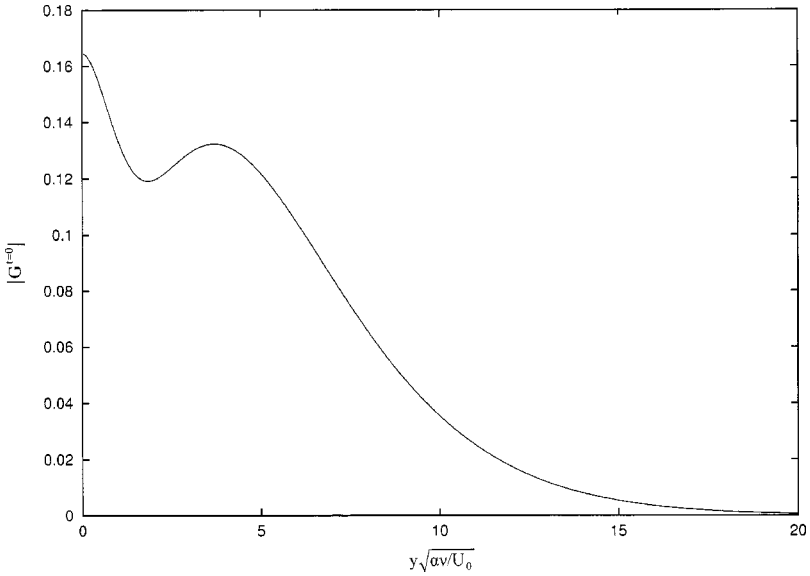

FIG. 9. Absolute value of the initial receptivity $G^{t=0}$ to stream function disturbances in the limit of $P\to0$, for t_M chosen equal to π.

given streamwise wave number, even though with decreasing wave number a larger and larger maximum amplification can be found at a larger and larger time. The marginal curve and curves of constant growth rate and frequency have been given here for the first time. The main conclusion of the stability work is that the effect of unsteadiness (nonparallelism in the corresponding spatial problem) is small. This conclusion entails that a unique functional form (a normal mode) exists for t sufficiently large, so that the objective of a receptivity study becomes the determination of the amplitude of this mode. An adjoint receptivity analysis is particularly well suited for this problem and, once proper care is taken of normalizing things appropriately, the Green's functions obtained by integrating the adjoint stability equation backward in time are of immediate interpretation and use. The wall Green's functions show the efficiency of arbitrary inhomogeneous wall conditions (roughness and blowing/suction) in triggering temporally growing Tollmien–Schlichting (TS) waves, whereas the initial Green's function gives the efficiency of whatever initial condition is exciting the instability. At the wall it is found that an excitation in the vertical component of the velocity is more effective than one in u; unsurprisingly, the largest response is found for excitations given at times close to the lower branch of the neutral stability curve. A very interesting result is that the initial receptivity is exceedingly small. If transposed to the spatial case, this would suggest that the leading-edge receptivity to TS waves in a Blasius boundary layer developing over an infinitely thin plate is negligible with respect to other receptivity mechanisms.

ACKNOWLEDGMENTS

We acknowledge Vincent Bourquin for several interesting discussions and for bringing Refs. 3–7 to our attention. P.L. was supported during his stay in Toulouse by Visiting Professorships awarded by the Université Paul Sabatier and by Institut National Polytechnique de Toulouse.

[1] H. Schlichting, *Boundary-Layer Theory* (McGraw-Hill, New York, 1979).
[2] R. L. Panton, *Incompressible Flow* (Wiley, New York, 1984).
[3] R. A. Hartunian, A. L. Russo, and P. V. Marrone, ''Boundary-layer transition and heat transfer in shock tubes,'' J. Aerosp. Sci. **27**, 587 (1960).
[4] R. E. Dillon, Jr. and H. T. Nagamatsu, ''Heat transfer and transition mechanism on a shock-tube wall,'' AIAA J. **22**, 1524 (1984).
[5] A. L. Myerson, Discussion on a paper by H. Mirels: ''Boundary layer growth effects in shock tubes,'' *Shock Tube Research, Proceedings of the 8th International Shock Tube Symposium*, Imperial College, London, 5–8 July 1971 (Chapman & Hall, London, 1971).
[6] T. Aoki, N. Kondoh, K. Matsuo, and S. Mashimo, ''Transition of unsteady boundary layer induced by propagating compression wave,'' *In Proceedings of the 20th International Symposium on Shock Waves* (World Scientific, Singapore, 1996), Vol. 1, p. 723.
[7] A. Pfeiffer, F. Ottisch, and H. Sockel, ''Experimental and theoretical investigation of two- and three-dimensional pressure waves propagating inside a tunnel due to a train passage,'' 8th International Symposium on the Aerodynamics and Ventilation of Vehicle Tunnels, Liverpool, UK, July 1994, p. 151.
[8] S. R. Otto, ''On the stability of a time dependent boundary layer,'' ICASE Report No. 93-73, 1993 (unpublished).
[9] J. C. Webb, S. R. Otto, and G. M. Lilley, ''On the nonlinear stability of viscous modes within the Rayleigh problem on an infinite flat plate,'' ICASE Report No. 94-30, 1994 (unpublished).
[10] H. Schlichting, ''Über die Stabilität der Couette-Strömung,'' Ann. Phys. V **14**, 905 (1932).
[11] N. Tillmark and P. H. Alfredsson, ''On Rayleigh instability in decaying plane Couette flow,'' Appl. Sci. Res. **53**, 187 (1994).
[12] M. Bouthier, ''Stabilité linéaire des écoulements presque parallèles,'' J. Mec. **11**, 599 (1972).
[13] M. Bouthien, ''Stabilité linéaire des écoulements presque parallèles. Partie II. La couche limite de Blasius,'' J. Mec. **12**, 75 (1973).
[14] M. Gaster, ''On the effects of boundary layer growth on flow stability,'' J. Fluid Mech. **66**, 465 (1974).
[15] W. S. Saric and A. H. Nayfeh, ''Nonparallel stability of boundary layer flows,'' Phys. Fluids **18**, 945 (1975).
[16] N. Itoh, ''The origin and subsequent development in space of Tollmien–Schlichting waves in a boundary layer,'' Fluid Dyn. Res. **1**, 119 (1986).
[17] F. P. Bertolotti, Th. Herbert, and P. R. Spalart, ''Linear and nonlinear stability of the Blasius boundary layer,'' J. Fluid Mech. **242**, 441 (1992).
[18] D. C. Hill, ''Adjoint systems and their role in the receptivity problem for boundary layers,'' J. Fluid Mech. **292**, 183 (1995).
[19] P. Luchini and A. Bottaro, ''Görtler vortices: A backward-in-time approach to the receptivity problem,'' J. Fluid Mech. **363**, 1 (1998).
[20] M. Van Dyke, *Perturbation Methods in Fluid Mechanics* (Parabolic, Stanford, 1975).
[21] W. Tollmien, ''Über die Entstehung der Turbulenz,'' Nachr. Ges. Wiss. Goettingen, Math.-Phys. Kl. 21 (1929); see also the discussion given in P. G. Drazin and W. H. Reid, *Hydrodynamic Stability* (Cambridge University Press, Cambridge, 1981), p. 165.
[22] R. Govindarajan and R. Narasimha, ''Low-order parabolic theory for 2D boundary-layer stability,'' Phys. Fluids **11**, 1449 (1999).
[23] J. D. Crouch, ''Localized receptivity of boundary layers,'' Phys. Fluids A **4**, 1408 (1992).
[24] A. Tumin, ''Receptivity of pipe Poiseuille flow,'' J. Fluid Mech. **315**, 119 (1996).
[25] D. E. Ashpin and E. Reshotko, ''The vibrating ribbon problem revisited,'' J. Fluid Mech. **213**, 531 (1990).
[26] F. P. Bertolotti, ''Receptivity of three-dimensional boundary layers to localized wall roughness and suction,'' Phys. Fluids **12**, 1799 (2000).
[27] G. B. Whitham, *Linear and Nonlinear Waves* (Wiley, New York, 1974).
[28] E. L. Ince, *Ordinary Differential Equations* (Dover, New York, 1944).
[29] P. M. Morse and H. Feshbach, *Methods of Theoretical Physics* (McGraw-Hill, New York, 1953).
[30] M. E. Goldstein, ''The evolution of Tollmien–Schlichting waves near a leading edge,'' J. Fluid Mech. **127**, 59 (1983).